Radiation pressure, absorption and AGN feedback in the Chandra Deep Fields

S. I. Raimundo[1]⋆, A. C. Fabian[1], F. E. Bauer[2], D. M. Alexander[3], W. N. Brandt[4], B. Luo[4], R. V. Vasudevan[4] and Y. Q. Xue[4]

[1] Institute of Astronomy, Madingley Road, Cambridge CB3 0HA
[2] Pontificia Universidad Católica de Chile, Departamento de Astronomía y Astrofísica, Casilla 306, Santiago 22, Chile
[3] Department of Physics, Durham University, Durham, DH1 3LE
[4] Department of Astronomy & Astrophysics, 525 Davey Lab, The Pennsylvania State University, University Park, PA 16802, USA

ABSTRACT
The presence of absorbing gas around the central engine of Active Galactic Nuclei (AGN) is a common feature of these objects. Recent work has looked at the effect of the dust component of the gas, and how it enhances radiation pressure such that dusty gas can have a lower effective Eddington limit than ionised gas. In this work, we use multi-wavelength data and X-ray spectra from the 2 Ms exposures of the *Chandra* Deep Field North and *Chandra* Deep Field South surveys, to characterise the AGN in terms of their Eddington ratio (λ) and hydrogen column density (N_H). Their distributions are then compared with what is predicted when considering the coupling between dust and gas. Our final sample consists of 234 objects from both fields, the largest and deepest sample of AGN for which this comparison has been made up to date. We find that most of the AGN in our sample tend to be found at low Eddington ratios (typically $10^{-4} < \lambda < 10^{-1}$) and high N_H ($>10^{22} \mathrm{cm}^{-2}$), with black hole masses in the range $\sim (10^8 - 10^9) M_{\odot}$. Their distribution is in agreement with that expected from the enhanced radiation pressure model, avoiding the area where we would predict the presence of outflows. We also investigate how the balance between AGN radiation pressure and gravitational potential influences the behaviour of clouds in the galactic bulge, and describe a scenario where an enhanced radiation pressure can lead to the fundamental plane of black hole/galaxy scaling relations.

Key words: galaxies: nuclei - galaxies: active - quasars: general - black hole physics

1 INTRODUCTION

Observations of Active Galactic Nuclei (AGN) have revealed that many of them are partially obscured by material in our line of sight, within the inner tens of parsecs of the central engine (e.g. Risaliti, Maiolino, & Salvati 1999 and Maiolino & Risaliti 2007 for a review). This obscuring material will influence both the AGN and our observations, and the study of its properties is fundamental for an unbiased understanding of AGN physics. The gas around the nucleus will be under the effect of the inward gravitational force of the supermassive black hole and the outward pressure of the radiation emitted in the central region. By investigating the balance between these two forces, one can predict the behaviour of the gas. The Eddington luminosity, L_E, is defined as the value at which the radiation pressure balances the gravitational force of the black hole: $L = L_E$, with $L_E = 4\pi G m_p c M_{BH}/\sigma_T$, where G is the gravitational constant, m_p the proton mass, c the speed of light, M_{BH}

the mass of the black hole and σ_T the cross-section for Thomson scattering. The Eddington ratio ($\lambda = L/L_E$), is then a measure of the balance between these two forces, for a certain M_{BH}. In the presence of dust, the gas couples with the dust grains via Coulomb interactions and the cross-section for the interaction with photons is considerable enhanced. The effective cross-section for dusty gas can be defined as $\sigma_d = A\sigma_T$ with a boost factor A (Fabian et al. 2006, Fabian, Vasudevan, & Gandhi 2008, Fabian et al. 2009). We can then determine an effective Eddington ratio for dusty gas as a function of the classical Eddington ratio:

$$\lambda_{\mathrm{eff}} = \frac{L\sigma_d}{4\pi G m_p c M_{BH}} = A\lambda.$$

It follows that, $\lambda = 1/A$ is now the limit at which the radiation pressure from the black hole is able to expel the mass of dusty gas around it. Fabian et al. (2008) and Fabian et al. (2009) explored the effective Eddington limit for dusty gas by investigating the properties of AGN samples in the *Chandra* Deep Field South (CDF-S), Lockman Hole and in the local Universe, and found that the objects tend to lie below their effective Eddington limit, as expected.

⋆ E-mail: sijr@ast.cam.ac.uk

AGN are expected to interact with the surrounding galaxy, affecting its evolution. In fact, there is evidence of a close interaction between galaxies and the supermassive black holes at their centres. Various studies have found correlations between the mass of the black hole and several properties of the galaxy when looking at samples in the local Universe. Kormendy & Richstone (1995) summarised the evidence for the presence of massive dark objects in the centres of galaxies and established a dependence between the masses of those objects and the galaxy luminosity/mass, a conclusion later strengthened by Magorrian et al. (1998) when looking at a larger sample of galaxies. Gebhardt et al. (2000) and Ferrarese & Merritt (2000) found that the black hole mass correlates with the velocity dispersion, and later on, correlations with other properties were determined (e.g.: Sérsic index - Graham et al. 2001). It has been suggested that these correlations are projections of a more fundamental relation or "fundamental plane". This argument is based on what is known for elliptical galaxies, where a fundamental plane was determined, involving the luminosity/effective radius, the velocity dispersion and the surface brightness (Dressler et al. 1987; Djorgovski & Davis 1987). Marconi & Hunt (2003), found evidence of a correlation between the residuals in the $M_{BH} - \sigma$ relation and the galaxy bulge effective radii. More recently, Hopkins et al. (2007) studied in detail the dependence of M_{BH} on the various galactic properties, establishing a fundamental plane of the form $M_{BH} \propto \sigma^{3.0\pm0.3} R^{0.43\pm0.19}$ or $M_{BH} \propto M_*^{0.54\pm0.17} \sigma^{2.2\pm0.5}$, reinforcing the idea of a very strong connection between the black hole and the evolution of the galaxy.

In this work we investigate how the radiation emitted by the AGN interacts with the obscuring gas around the central black hole, and determine how this affects the structure of the host galaxy. We start by determining the obscuration properties of a large sample of AGN detected in the deepest X-ray surveys of the *Chandra* Deep Field North (CDF-N) (Alexander et al. 2003) and *Chandra* Deep Field South (CDF-S) (Luo et al. 2008). The properties of our objects are then compared with predictions from the enhanced radiation pressure model, as in Fabian et al. (2008) and Fabian et al. (2009), but with a deeper exposure, to enable the analysis of a larger number of AGN and a better signal to noise ratio in the X-ray spectral analysis. Finally, we investigate the role of the radiation/dusty gas interaction in the properties of the host galaxy, namely, on establishing the scaling relations between the black hole and the galaxy. We adopt standard cosmological parameters of $H_0 = 70$ km s^{-1} Mpc^{-1}, $\Omega_m = 0.27$ and $\Omega_\Lambda = 0.73$.

2   DATA ANALYSIS

To compare the data with the dusty gas model, we used the point sources found with the 2 Ms exposure in the CDF-N (Alexander et al. 2003) and the 2 Ms exposure in the CDF-S (Luo et al. 2008). Spectroscopic redshifts for the CDF-S were collected by Luo et al. (2010) and by Rafferty et al. (2010) for the CDF-N. Photometric redshifts for the CDF-S are also from Luo et al. (2010), with a typical accuracy of $|\Delta z|/(1 + z) \approx 7\%$, and from Xue et al. (2010) for the CDF-N, with an accuracy of $\approx 11\%$. X-ray spectra for our sample were extracted from the CDF-N and CDF-S datasets using the IDL routine ACIS *Extract* (Broos et al. 2010), which incorporates several advancements over standard CIAO procedures. The spectra were fitted in XSPEC (v12.2.1o; Arnaud 1996) with an absorbed powerlaw model tbabs(ztbabs+pegpwrlw), allowing the photon index to change and with the normalisation determined by the 0.5-8 keV
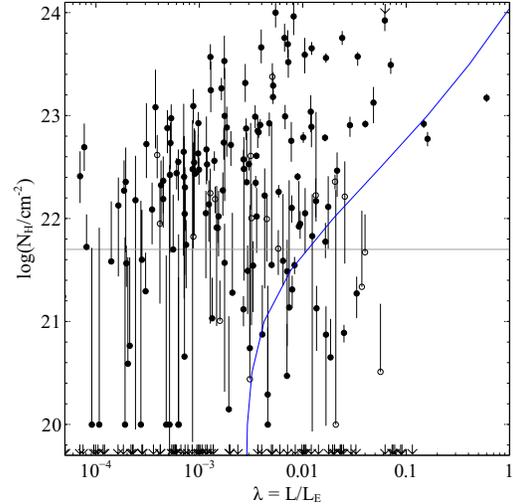

Figure 1. Hydrogen column density (N$_H$) versus Eddington ratio (λ), for AGN with $z < 1$. The filled circles represent objects with measured spectroscopic redshifts and the open circles objects with photometric redshifts. The downward arrows point to the Eddington ratios of objects with negligible absorption (log N$_H$ $\sim$ 19.0). The blue line represents the effective Eddington limit when accounting for the presence of dust, and the horizontal grey line is an approximate limit for the column density of a dust lane (N$_H$ $\sim$ 5×10^{21} cm^{-2}). Outflows or transient absorption are expected to happen above the limit for dust lanes and to the right of the blue line. Objects tend to lie in the upper left region of the plot, with high column densities, avoiding the outflow area. The vertical error bars represent the 1σ deviations in N$_H$. Errors in λ are of the order of 30%.

observed flux. The pegpwrlw model was used to allow an unbiased determination of the normalisation. A full account of the spectral analyses of the CDF sources will be presented in Bauer et al. 2010 (in prep). Objects for which the best-fitted parameters tended to extreme non-physical values were excluded, (for example, when the two fitting parameters, Γ and N_H tend to the limits imposed in the fit), since this is an indication that the model adopted does not provide an accurate description of the data. The X-ray intrinsic (absorption corrected) luminosity in the 2-10 keV band for each source, was obtained from the spectral fit parameters and used to identify AGN: we select objects with $L_X > 10^{41}$ erg s^{-1}, since the X-ray emission can be contaminated by star formation in lower luminosity sources. The value of hydrogen column density (N_H) was obtained from the X-ray spectral fitting with the models described above.

To obtain the Eddington ratio for the AGN, the bolometric luminosity and the mass of the black hole are needed. The X-ray luminosities in the 2-10 keV band were converted to bolometric luminosities using a bolometric correction of 19 for objects with an X-ray photon index, Γ, lower than 1.9 and a correction of 55 otherwise, as done in Fabian et al. (2009). This correction is based on Winter et al. (2008), where a correlation is found between Γ and Eddington ratio in various observations of individual objects. The total absolute rest-frame K-band magnitude of the galaxy was obtained by Xue et al. (2010) from SED fitting. This value was corrected for the nuclear emission from the AGN using an X-ray luminosity and N_H dependent scaling factor (Eq. 1 from Vasudevan et al. 2009), and we consider that the galaxy host K-band light is dominated by the bulge, following studies which found AGN hosts to be typically early type galaxies (Kauffmann et al. 2003) with bulge dominated morphologies
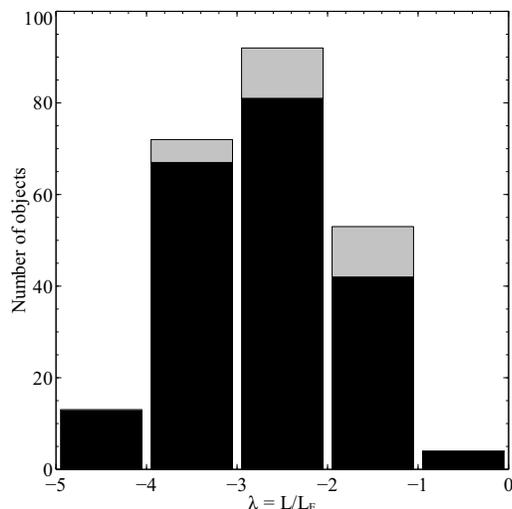
Figure 2. Number of objects with $z < 1$ binned in terms of their Eddington ratios (λ). Black histogram represents sources with spectroscopic redshifts, grey histogram adds the sources with photometric redshifts only. AGN have a wide range of Eddington ratios, varying mainly between $10^{-4} - 10^{-1}$, as also found by Babić et al. (2007).
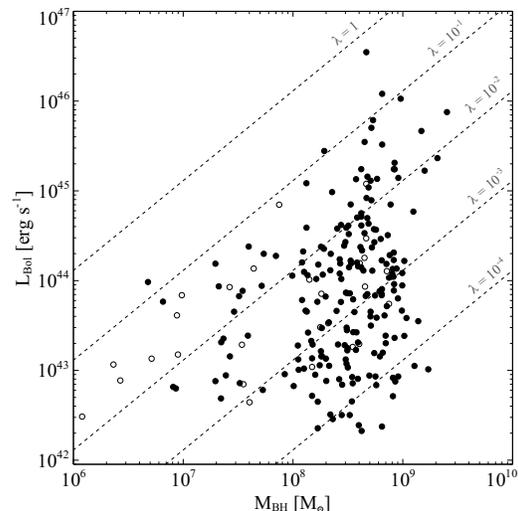

Figure 3. Bolometric luminosity as a function of mass for every AGN with $z < 1$. The filled circles represent AGN with measured spectroscopic redshifts and the open circles AGN with photometric redshifts only. The dashed lines separate between different Eddington ratios. Most of the AGN have $M_{BH} \sim (10^8 - 10^9) M_\odot$.

(Grogin et al. 2005). This may however be a simplification, a recent study showed that X-ray selected AGN hosts show a broad range of morphologies, with an intermediate distribution between bulge and disc dominated galaxies (Gabor et al. 2009). The masses were obtained using the scaling relation between the black hole mass and the bulge absolute K-band magnitude: $\log(M_{BH}/M_\odot) = -0.37(\pm0.04)(M_K+24)+8.29(\pm0.08)$ (Graham 2007). The possible evolution of the relation between black hole mass and K-band magnitude will be discussed in section 3.1.

The objects in our sample were selected from both *Chandra* Fields, and have redshifts $z < 1$. There are 253 AGN with measured K-band magnitudes and redshifts below one. Out of these, 19 are excluded due to problems in the fit (fitting parameters converging to extreme values). In summary we have a sample of 234 AGN, out of which 207 have spectroscopic redshifts and 27 have photometric redshifts.

3 DISCUSSION

We plot our results in Fig. 1 in the same way as in Fabian et al. (2008) and Fabian et al. (2009). The blue line represents the effective Eddington limit for dusty gas, obtained using CLOUDY (details in Fabian et al. 2006, Fabian et al. 2008). We expect the objects to the right of the line to have outflows or to have the absorbing gas further away from the central black hole, so that they are under the effect of a larger gravitational mass. If they are associated with dust lanes, (e.g. Matt 2000), the N_H value will not be intrinsic AGN absorption only, it will be caused by gas further out in the galaxy as well. If there is a dust lane, its mass of gas has a maximum limit, so the column density cannot be larger than a certain value. We use as reference the value of $N_H = 5 \times 10^{21} \text{cm}^{-2}$ as in Fabian et al. (2008) and plot it in Fig. 1 as a grey horizontal line. To the right of the blue line and above the grey line, we expect to have objects experiencing outflows or variable absorption. The Compton-thick objects ($N_H \gtrsim 1.5 \times 10^{24} \text{cm}^{-2}$) never see the source above the effective Eddington limit, so their absorption is

long-lived for $\lambda < 1$. Most of our objects lie in the upper left region of the plot, with a high column density ($\log N_H \gtrsim 22$) and low Eddington ratio ($\lambda \lesssim 10^{-1}$). More than 95% of the sources with $\log N_H > 5 \times 10^{21} \text{cm}^{-2}$ avoid the area where we would expect to see outflows (to the right of the blue line and above the horizontal grey line), which means that the absorbing clouds around them are long-lived. Considering the error bars, there are only two objects with an Eddington ratio clearly above the effective Eddington limit. This is unlikely to be a selection effect, since for a given M_{BH} the sources with higher Eddington ratios should be in general easier to detect.

We explored the effects of using different bolometric corrections. Both a constant bolometric correction of ~ 30, or an Eddington ratio dependent bolometric correction (Vasudevan & Fabian 2007) reproduce the same general properties as deduced from Fig. 1. The position of the points change relatively, but there are only two clear points with $N_H > 5 \times 10^{21} \text{cm}^{-2}$ above the effective Eddington limit and those are the same objects as in Fig. 1. The Eddington ratio distribution of our sample ($z < 1$) can be seen in Fig. 2. It peaks at around ($10^{-3} - 10^{-2}$) with most of the sources having Eddington ratios between ($10^{-4} - 10^{-1}$) in agreement with what was found by Babić et al. (2007) when looking at AGN in the CDF-S. In summary, our sample can be characterised in terms of its overall properties in Fig. 3; the black hole mass for the majority of the sources is in the range $M_{BH} \sim (10^8 - 10^9) M_\odot$, with bolometric luminosity $L_{bol} \sim (10^{42} - 10^{45}) \text{erg s}^{-1}$ and relatively low Eddington ratio. We obtained black hole masses that are in general higher than the ones found in Ballo et al. (2007), the majority of their sources have $M_{BH} \sim (10^7 - 10^{8.5}) M_\odot$. This discrepancy can be partially explained by the different scaling relation adopted in their work: the R-band magnitude relation from McLure & Dunlop (2002), which yields a conservative lower limit for the black hole masses.
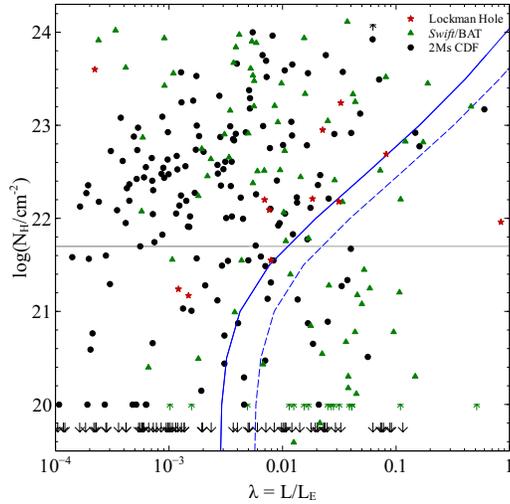
Figure 4. Hydrogen column density (N_H) versus Eddington ratio (λ) summary plot of results from the Lockman Hole (Fabian et al. 2008), *Swift*/BAT (Fabian et al. 2009) and 2 Ms *Chandra* Deep Fields (this work). Sources from the 9 month *Swift*/BAT catalogue of local AGN are represented with green triangles, Lockman Hole with red stars, and black circles for the AGN in the *Chandra* Deep Fields. Upward arrows are upper limits for some of the objects in the *Swift*/BAT catalogue. The dashed blue line considers the mass of intervening stars when calculating the effective Eddington limit.

3.1 Comparison with other samples

We compared our results with those previously found by Fabian et al. (2008) and Fabian et al. (2009). These authors looked at local samples of AGN from the *Swift*/BAT survey (Winter et al. 2008), and higher redshift ($0.5 < z < 1$) samples from the Lockman Hole (Mainieri et al. 2002; Mateos et al. 2005) and from the 1 Ms exposure in the CDF-S (Tozzi et al. 2006). In Fig. 4, we compile the results from the present work, Fabian et al. (2008) and Fabian et al. (2009). The 1 Ms CDF-S results are excluded due to our current analysis of a deeper observation in this field (2 Ms). For the gas further away from the black hole, (hundreds of parsecs to kpc), the enclosed mass will include stars, and the effective Eddington limit will be higher. We follow Fabian et al. (2009) and plot a dashed line to indicate a factor of two increase in the enclosed mass. Analysing all the results, with a larger number of sources at different redshifts, we obtain the same conclusions stated previously: the AGN tend to avoid the area where outflows are expected (in the upper right corner of the plot). More than 90% of the sources with log $N_H > 5 \times 10^{21}$cm^{-2} are located to the left of the solid blue line, and more than 98% lie to the left of the dashed blue line.

We also limited our sample to log $L_X > 41.5$, to have approximately the same range of X-ray luminosities as the AGN in the *Swift*/BAT study of Winter et al. (2009), and to be able to compare some of our $z < 1$ sample properties with what is found for their local AGN. The fraction of absorbed sources (log $N_H > 22$) and the fraction of highly absorbed sources (log $N_H > 23$) as a function of the X-ray Eddington ratio are plotted in Fig. 5. The absorbed AGN constitute, in general, the largest fraction of sources, as found in the local sample of Winter et al. (2009). The fraction of absorbed sources at low λ_X is nevertheless lower than in the local sample, but this is due to the fact that the *Swift*/BAT sample has more obscured AGN at low luminosities than our own (Mullaney et al. 2010).

From our study, we predict a decrease in the fraction of obscured objects with increasing Eddington ratio, in particular for the
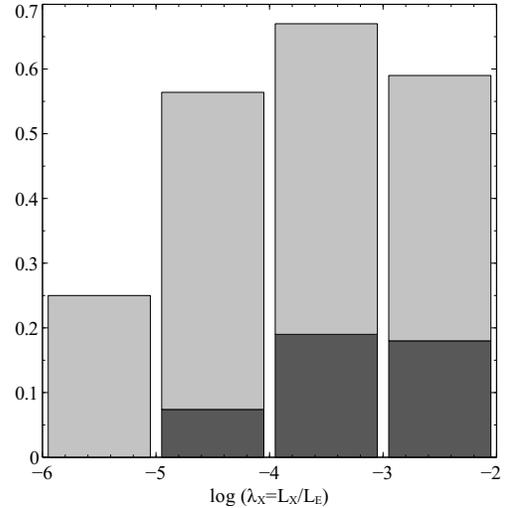

Figure 5. Fraction of objects binned as a function of their X-ray Eddington ratio (λ_X). The light grey histogram represents the fraction of sources with log $N_H > 22$ and the dark grey sources with log $N_H > 23$.

highest values of λ. This trend would be seen for objects with log $N_H \sim 21.5 - 23$, due to a decrease in the number of AGN above their effective Eddington limit, but would be weaker/disappear for the higher column densities log $N_H \gtrsim 23.5$. If we assume a typical black hole mass of $10^8 M_\odot$, this means that with our boundary region, we are predicting a decrease in the fraction of log $N_H \sim 21.5 - 23$ objects for luminosities higher than $L_X \approx 3 \times 10^{43}$erg s^{-1}. The AGN obscuration fraction has been investigated many times, and recently with XMM observations in the COSMOS field by Brusa et al. (2010). They show a decrease in the fraction of obscured sources with increasing luminosity above $L_X \sim 3 \times 10^{43}$erg s^{-1}, in agreement with previous work on this subject (e.g. Ueda et al. 2003; Hasinger 2008) and the reasoning above.

Several authors have studied the evolution with redshift of galaxy scaling relations. Peng et al. (2006) found that the observed $M_{BH} - L_R$ relation evolves with redshift for a sample of $1.7 < z < 4.5$ AGN, but it is consistent with no evolution when looking at lower redshift objects ($z < 1.7$). Treu et al. (2007) investigates this trend using observations of 20 Seyfert galaxies at $z = 0.36$, and finds an evolution in the $M_{BH} - L_B$ scaling relation. More recently, Merloni et al. (2010) studied a sample of type-1 AGN from the zCOSMOS survey in the redshift range $1 < z < 2.2$, and concluded that the objects at higher redshift tend to be brighter in the K-band for a given black hole mass, than the local ones. The amount of evolution in the black hole/galaxy scaling relations is still arguable, but we aim to evaluate the effect of such evolution in our mass estimates. Considering the trend found in Merloni et al. (2010), we correct our K-band luminosities by a factor $-0.73 \log(1+z)$. Our mass estimates will then be: $\log(M_{BH}/M_\odot) = -0.37(\pm 0.04)(M_K + 2.5 \times 0.73 \log(1+z) + 24) + 8.29(\pm 0.08)$, which means that at our highest redshift ($z = 1$), M_{BH} is ~ 1.6 times lower than the estimate using the local scaling relation. As we can see in Fig. 6, these lower values for the M_{BH} cause the Eddington ratios to be higher, but the main conclusions of the present work remain the same. Note that the scaling found in Merloni et al. (2010) is valid for more luminous and higher redshift sources than our sample. Our analysis is indicative of how the results are affected by a redshift evolution, but is subject to uncertainties related
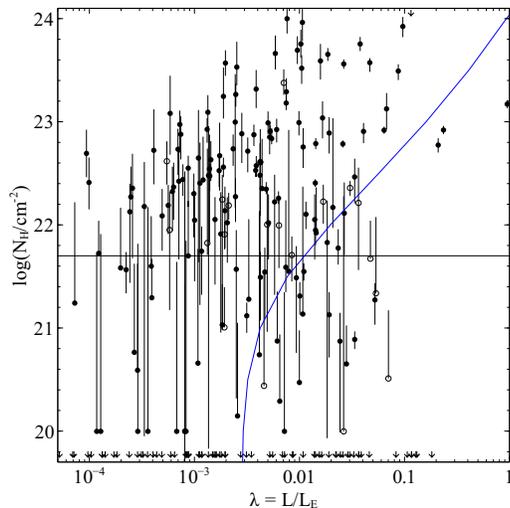
Figure 6. Similar to Fig. 1, but considering a redshift evolution in the black hole mass - galaxy scaling relation from Merloni et al. (2010).

Figure 7. Approximate parameter space covered by studies of luminous quasars. Light grey region represents quasars selected in the mid-IR, while the dark grey shows area covered by optical identification of luminous quasars. Crosses represent low redshift quasars from the work of Inoue et al. (2007), showing signs of outflows in their spectra.

with the precise form of the evolution for our type of sources. The redshift evolution of the radiation pressure and gas interaction itself is still hard to constrain. We are limited by selection biases: low luminosity AGN are not detected at high redshifts and gas/dust can obscure luminous objects beyond our detectability limit. We hope to be able to determine how objects evolve in the N_H vs λ plot with future X-ray surveys. The planned *International X-Ray Observatory* (IXO), will be able to detect AGN outflows at high redshifts, due to its high spectral resolution at low X-ray energies (< 2 keV) and large effective area, by measuring the blueshift of narrow absorption lines. The sources lying close to the effective Eddington limit in our plot, and in particular, the ones clearly above that limit, are good targets for future spectroscopic studies like those.

3.2 High Eddington ratio

Most of our objects lie below $\lambda \sim 0.1$ which means that the range of high Eddington ratios is not fully probed by the CDF AGN. To sample the area of $\lambda \gtrsim 0.1$ requires that we look at the regions probed by investigations of the rarer luminous quasars (Fig. 7). Kollmeier et al. (2006) and Steinhardt & Elvis (2010) show that the most luminous objects in the SDSS have $\lambda \sim 0.2 - 0.3$, but do not investigate any absorption properties. Greene et al. (2009) look at a large sample of narrow line AGN, and find that they have high Eddington ratios (~ 0.2). Although these sources are obscured, there are no available values for their hydrogen column densities. Just et al. (2007) do study the X-ray properties of 59 of the most optically luminous quasars and find that each is consistent with no intrinsic absorption and collectively are obscured by a mean column density $< 2 \times 10^{21}$cm^{-2}. For typical values of $L_X \gtrsim 10^{45}$, and imposing a maximum value of 10^{10}M$_\odot$ for the black hole mass, the minimum value for λ is ~ 0.04. The study of optically luminous quasars covers the area of high Eddington ratios but mildly obscured objects (the dark grey region in Fig. 7). Another study of luminous quasars by Shemmer et al. (2008) gives upper limits for the hydrogen column density for five luminous high redshift quasars and concludes that N_H is lower than $3 \times 10^{21} - 4 \times 10^{22}$cm^{-2}. As in Just et al. (2007), they find no significant absorption in their sources, with the data being consistent with zero intrinsic absorp-
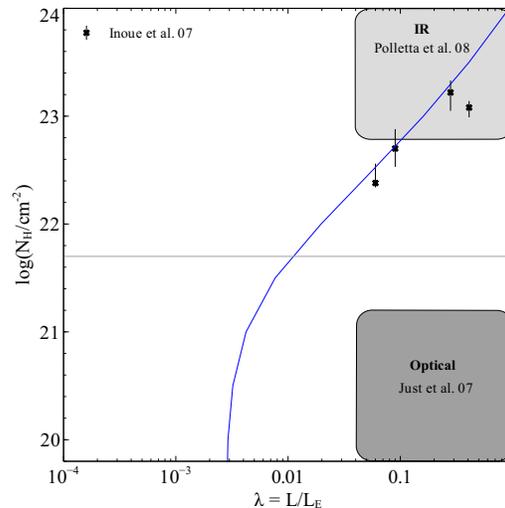
tion. On the other hand, infrared-selected luminous quasars cover the high N_H range. Polletta et al. (2008) investigate the obscuration properties of luminous quasars selected in the mid-infrared and, using X-ray measurements, determine the column density for five of them. Their bolometric luminosity is $\sim 10^{46} - 10^{47}$erg s^{-1}, and with the same assumptions as above, the Eddington range probed is $\gtrsim 0.04$. The column densities are higher than $N_H = 6.3 \times 10^{22}$cm^{-2} for four of the objects, populating the light grey area plotted in Fig. 7, while the fifth lies in the Just et al. (2007) region. We also plot data from Inoue, Terashima, & Ho 2007, on low redshift quasars, for which λ and N_H values are available. These objects have $L \gtrsim 10^{45}$, and tend to lie close to the effective Eddington limit boundary. As predicted in the enhanced radiation pressure model, they show the presence of outflows in the UV (Brandt et al. 2000; Laor & Brandt 2002). Individual X-ray spectroscopic studies of these quasars have found the presence of warm absorbers (ionised material): Piconcelli et al. (2004) for PG 2214+139, Brinkmann, Papadakis, & Ferrero (2004) also for PG 2214+139 and PG 1411+442, Miller et al. (2006) for the broad absorption line quasar PG 1004+130 and by Schartel et al. (2005) and Ballo et al. (2008) for PG 1535+547. In summary, the N_H sampling of the high Eddington ratio region is not as good as for the low Eddington ratios. We have found no objects in the region bounded by $2 \times 10^{21} \lesssim N_H \lesssim 4 \times 10^{22}$cm^{-2} and $\lambda > 0.04$ which do not show outflows, in agreement with enhanced radiation pressure arguments. There are possible selection effects on probing this region, optical measurements are affected by reddening so they might not be immediately selected as bright quasars, yet the column densities may be too low for them to be selected in the infrared.

3.3 Radiation pressure effect on the bulge of the galaxy

In the scenario described in the previous sections, one can investigate the interaction between the enhanced radiation pressure and the dusty gas, and what is the long term effect on the bulge of the galaxy. If we start by considering the Eddington luminosity for

dusty gas, we have:

$$L_{E_d} = \frac{4\pi G m_p c M_{BH}}{\sigma_d}$$

which is σ_d/σ_T times lower than the Eddington luminosity for Thomson scattering. Considering a scenario where the gas is concentrated in a shell at the edge of the galaxy of radius R, after being swept out by a quasar at its effective Eddington limit (Fabian 2009), we can balance the radiation pressure and the gravitational force:

$$\frac{L_{E_d}}{c} = \frac{G M_{gal} M_{gas}}{R^2}$$

The mass of gas will be a fraction f of the galaxy mass, and the effective Eddington ratio will now include the mass of the entire galaxy ($M_{\rm gal} \gg M_{\rm BH}$):

$$\frac{4\pi G m_p M_{gal}}{\sigma_d} \sim \frac{G f M_{gal}^2}{R^2}$$

Solving this equation in order to determine M_{gal}, and assuming an isothermal galaxy, with $M_{gal} = 2\sigma^2 R/G$, where σ is the velocity dispersion of the galaxy and R the radius:

$$M_{gal} \sim \frac{4\pi m_p R^2}{f \sigma_d} \sim \frac{2\sigma^2 R}{G} \tag{1}$$

$$M_{gal} \sim \frac{f \sigma^4 \sigma_d}{\pi m_p G^2}. \tag{2}$$

The mass of the black hole correlates with the velocity dispersion of the galaxy: $M_{\rm BH} \propto \sigma^4$, and it can be explained based on momentum balance arguments (Fabian 1999; Fabian et al. 2002; King 2003; Murray et al. 2005). Using Eq. 2 and the latter correlation, we obtain a relation between the mass of the galaxy and the mass of the black hole: $M_{\rm BH}/M_{\rm gal} \propto \sigma_d^{-1}$. The effective cross-section (σ_d) is expected to decrease at higher redshifts, when the dust content in the tens of parsecs scale is lower, (see Fabian et al. 2009 for details on how σ_d/σ_T changes with metallicity) in agreement with studies that find an increase in the $M_{\rm BH}/M_{\rm gal}$ fraction at higher redshifts (e.g.: Merloni et al. 2010). From Eq. 1, we obtain (Fabian 2009):

$$\frac{\sigma^2}{R} \sim \frac{2\pi m_p G}{f \sigma_d}$$

which indicates a relation between the velocity dispersion and the radius of the galaxy, implying a close interaction between the feedback from the AGN and the large scale properties of the galaxy. This relation is also in agreement with the dependency observed in terms of a fundamental plane (Hopkins et al. 2007), where if $M_{\rm BH} \propto \sigma^4$, then $\sigma^2 \propto R$.

4   CONCLUSIONS

We have examined the absorption column densities and Eddington fraction distributions of a large sample of AGN from the CDF-N and CDF-S fields. These objects tend to lie below their effective Eddington limit for dusty gas, with more than 95 per cent of AGN with $N_{\rm H} > 5 \times 10^{21} {\rm cm}^{-2}$, being sub-Eddington in that sense. This conclusion is in agreement with previous results, applicable to not only $z \sim (0.5 - 1.0)$ AGN but also to local samples. Future spectroscopic studies should find outflows at the effective Eddington limit boundary. Our results are consistent with the action of radiation pressure on the dusty interstellar gas within the inner 100

pc or so of the host galaxy. Much deeper studies of the rarer objects near the effective Eddington limit are required to determine the role this mechanism plays in AGN feedback. It must occur, but the effect of transient jets or fast winds could be greater. The lack of a significant population above the limit indicates that large amplitude changes in λ on timescales less than the gas expulsion time ($\sim 10^5$ yr) are rare. The overall evolution of AGN in the λ vs $N_{\rm H}$ plane is unclear, although it is likely that an active phase is initiated when gas is plentiful and thus at high $N_{\rm H}$. If AGN exceed the effective Eddington limit, they expel much of their fuel supply (except what remains in the accretion disk) and so are likely to be short lived ($\lesssim 10^7$ yr).

In this work, we have also suggested a possible galaxy evolution scenario in line with what is observed. The effective cross-section for dusty gas can be up to a factor ~ 1000 higher than that for Thomson scattering, resulting in an enhanced radiation pressure capable of exceeding the gravitational force of the gas clouds around the AGN. The interaction between these two forces affects the gas content of the host galaxy, resulting in correlations between the black hole and the host galaxy, which will ultimately lead to a "fundamental plane" relation.

REFERENCES

Alexander D. M. et al., 2003, AJ, 126, 539
Arnaud K. A., 1996, in Astronomical Society of the Pacific Conference Series, Vol. 101, G. H. Jacoby & J. Barnes , ed, Astronomical Data Analysis Software and Systems V, p. 17
Babić A., Miller L., Jarvis M. J., Turner T. J., Alexander D. M., Croom S. M., 2007, A&A, 474, 755
Ballo L. et al., 2007, ApJ, 667, 97
Ballo L., Giustini M., Schartel N., Cappi M., Jiménez-Bailón E., Piconcelli E., Santos-Lleó M., Vignali C., 2008, A&A, 483, 137
Brandt W. N., Laor A., Wills B. J., 2000, ApJ, 528, 637
Brinkmann W., Papadakis I. E., Ferrero E., 2004, A&A, 414, 107
Broos P. S., Townsley L. K., Feigelson E. D., Getman K. V., Bauer F. E., Garmire G. P., 2010, ArXiv e-prints, 1003.2397
Brusa M. et al., 2010, ArXiv e-prints 1004.2790
Djorgovski S., Davis M., 1987, ApJ, 313, 59
Dressler A., Lynden-Bell D., Burstein D., Davies R. L., Faber S. M., Terlevich R., Wegner G., 1987, ApJ, 313, 42
Fabian A. C., 1999, MNRAS, 308, L39
Fabian A. C., 2009, ArXiv e-prints 0912.0880
Fabian A. C., Celotti A., Erlund M. C., 2006, MNRAS, 373, L16
Fabian A. C., Vasudevan R. V., Gandhi P., 2008, MNRAS, 385, L43
Fabian A. C., Vasudevan R. V., Mushotzky R. F., Winter L. M., Reynolds C. S., 2009, MNRAS, 394, L89

Fabian A. C., Wilman R. J., Crawford C. S., 2002, MNRAS, 329, L18

Ferrarese L., Merritt D., 2000, ApJ, 539, L9

Gabor J. M. et al., 2009, ApJ, 691, 705

Gebhardt K. et al., 2000, ApJ, 539, L13

Graham A. W., 2007, MNRAS, 379, 711

Graham A. W., Erwin P., Caon N., Trujillo I., 2001, ApJ, 563, L11

Greene J. E., Zakamska N. L., Liu X., Barth A. J., Ho L. C., 2009, ApJ, 702, 441

Grogin N. A. et al., 2005, ApJ, 627, L97

Hasinger G., 2008, A&A, 490, 905

Hopkins P. F., Hernquist L., Cox T. J., Robertson B., Krause E., 2007, ApJ, 669, 67

Inoue H., Terashima Y., Ho L. C., 2007, ApJ, 662, 860

Just D. W., Brandt W. N., Shemmer O., Steffen A. T., Schneider D. P., Chartas G., Garmire G. P., 2007, ApJ, 665, 1004

Kauffmann G. et al., 2003, MNRAS, 346, 1055

King A., 2003, ApJ, 596, L27

Kollmeier J. A. et al., 2006, ApJ, 648, 128

Kormendy J., Richstone D., 1995, ARA&A, 33, 581

Laor A., Brandt W. N., 2002, ApJ, 569, 641

Luo B. et al., 2008, ApJS, 179, 19

Luo B. et al., 2010, ApJS, 187, 560

Magorrian J. et al., 1998, AJ, 115, 2285

Mainieri V., Bergeron J., Hasinger G., Lehmann I., Rosati P., Schmidt M., Szokoly G., Della Ceca R., 2002, A&A, 393, 425

Maiolino R., Risaliti G., 2007, in Astronomical Society of the Pacific Conference Series, Vol. 373, L. C. Ho & J.-W. Wang , ed, The Central Engine of Active Galactic Nuclei, p. 447

Marconi A., Hunt L. K., 2003, ApJ, 589, L21

Mateos S., Barcons X., Carrera F. J., Ceballos M. T., Hasinger G., Lehmann I., Fabian A. C., Streblyanska A., 2005, A&A, 444, 79

Matt G., 2000, A&A, 355, L31

McLure R. J., Dunlop J. S., 2002, MNRAS, 331, 795

Merloni A. et al., 2010, ApJ, 708, 137

Miller B. P., Brandt W. N., Gallagher S. C., Laor A., Wills B. J., Garmire G. P., Schneider D. P., 2006, ApJ, 652, 163

Mullaney J. R., Alexander D. M., Huynh M., Goulding A. D., Frayer D., 2010, MNRAS, 401, 995

Murray N., Quataert E., Thompson T. A., 2005, ApJ, 618, 569

Peng C. Y., Impey C. D., Rix H., Kochanek C. S., Keeton C. R., Falco E. E., Lehár J., McLeod B. A., 2006, ApJ, 649, 616

Piconcelli E., Jimenez-Bailón E., Guainazzi M., Schartel N., Rodríguez-Pascual P. M., Santos-Lleó M., 2004, MNRAS, 351, 161

Polletta M., Weedman D., Hönig S., Lonsdale C. J., Smith H. E., Houck J., 2008, ApJ, 675, 960

Rafferty D. A., others , 2010, ApJ, submitted

Risaliti G., Maiolino R., Salvati M., 1999, ApJ, 522, 157

Schartel N., Rodríguez-Pascual P. M., Santos-Lleó M., Clavel J., Guainazzi M., Jiménez-Bailón E., Piconcelli E., 2005, A&A, 433, 455

Shemmer O., Brandt W. N., Netzer H., Maiolino R., Kaspi S., 2008, ApJ, 682, 81

Steinhardt C. L., Elvis M., 2010, MNRAS, 402, 2637

Tozzi P. et al., 2006, A&A, 451, 457

Treu T., Woo J., Malkan M. A., Blandford R. D., 2007, ApJ, 667, 117

Ueda Y., Akiyama M., Ohta K., Miyaji T., 2003, ApJ, 598, 886

Vasudevan R. V., Fabian A. C., 2007, MNRAS, 381, 1235

Vasudevan R. V., Mushotzky R. F., Winter L. M., Fabian A. C., 2009, MNRAS, 399, 1553

Winter L. M., Mushotzky R. F., Reynolds C. S., Tueller J., 2009, ApJ, 690, 1322

Winter L. M., Mushotzky R. F., Tueller J., Markwardt C., 2008, ApJ, 674, 686

Xue Y. Q., others , 2010, ApJ, submitted